

Hyperfine structure and isotopic shift of the n^2P_J levels ($n = 7-10$) of $^{203,205}\text{Tl}$ measured by Doppler-free two-photon spectroscopy

M. Grexa, G. Hermann, and G. Lasnitschka

I. Physikalisches Institut, Justus-Liebig-Universität Giessen, D-6300 Giessen, Federal Republic of Germany

B. Fricke

Fachbereich Physik, Gesamthochschule Kassel, D-3500 Kassel, Federal Republic of Germany

(Received 25 January 1988)

Using Doppler-free two-photon absorption spectroscopy, we have measured hyperfine splitting constants as well as isotopic level shifts of the $6s^2np^2P_{1/2,3/2}$ states ($n = 7-10$) in ^{203}Tl and ^{205}Tl . Calculations for hyperfine constants and electron density at the nucleus have been performed by the Dirac-Fock method. The experimental results are compared with these calculations as well as with the predictions of the semiempirical theory.

I. INTRODUCTION

Thallium is a group III element with an electron configuration characterized by a single p electron outside closed shells. In the ground state, the electron configuration is $5s^25p^65d^{10}6s^26p$. Figure 1 shows an energy-level diagram of the $nP_{1/2}$ and $nP_{3/2}$ states in Tl I with term energies as tabulated.¹

There are two stable isotopes, ^{203}Tl and ^{205}Tl , with natural abundances of 30% and 70%, respectively, both with a nuclear spin $I = 1/2$. Thus only magnetic hyperfine interaction has to be considered. Because of the single-valence-electron configuration of thallium, the semiempirical theory of hyperfine interaction seems to be a suitable tool to describe the hyperfine splittings (HFS's) of the atomic levels. Since thallium ($Z = 81$) is a heavy element, the HFS data are well suited to test relativistic corrections of the semiempirical theory. In addition, relativistic Dirac-Fock calculations were carried out mainly for the isotopic shift (IS) but also for the radial parameters of hyperfine structure.

HFS and the IS in the n^2P_J states of thallium have been studied experimentally during the last three decades by various methods. While for $n = 6$ HFS radiofrequency measurements^{2,3} are available with high accuracy (errors less than 1 kHz), no values for the IS have been measured with comparable accuracy (errors of 40 MHz).^{4,5} In 1960 Odintsov⁴ measured HFS and the IS in some levels of the nP_J series ($6P_{3/2}, 8P_J, 9P_J, 10P_{3/2}$) by classical optical-interference spectroscopy with errors of at least 15 MHz. Doppler-free two-photon spectroscopy has already been applied for HFS and line-IS measurements of the $6P_{1/2} - 7P_{1/2,3/2}$ transitions,⁶ but the accuracy obtained was not better than that of Odintsov. In addition, level-IS data had to be referenced to Odintsov's measurements. New results for the HFS of the $10P_{3/2}$ state, the $6P_J$ and $7P_J$ states, and the line IS have been published recently^{7(a)7(b)} also using Doppler-free two-photon spectroscopy.

For higher $nP_{3/2}$ states ($n = 10-13$) the HFS of ^{205}Tl measured by two-photon quantum-beat spectroscopy

with errors less than 1 MHz has been published in a previous paper⁸ and some preliminary experimental results for the levels $n = 7, 8, 9$ have already been presented in a short note.⁹ The measurements reported previously¹⁰ give the HFS of both isotopes for all nP_J terms ($n = 7-10$) of both stable isotopes $^{203,205}\text{Tl}$ within experimental-error limits of 1 MHz. Furthermore, the

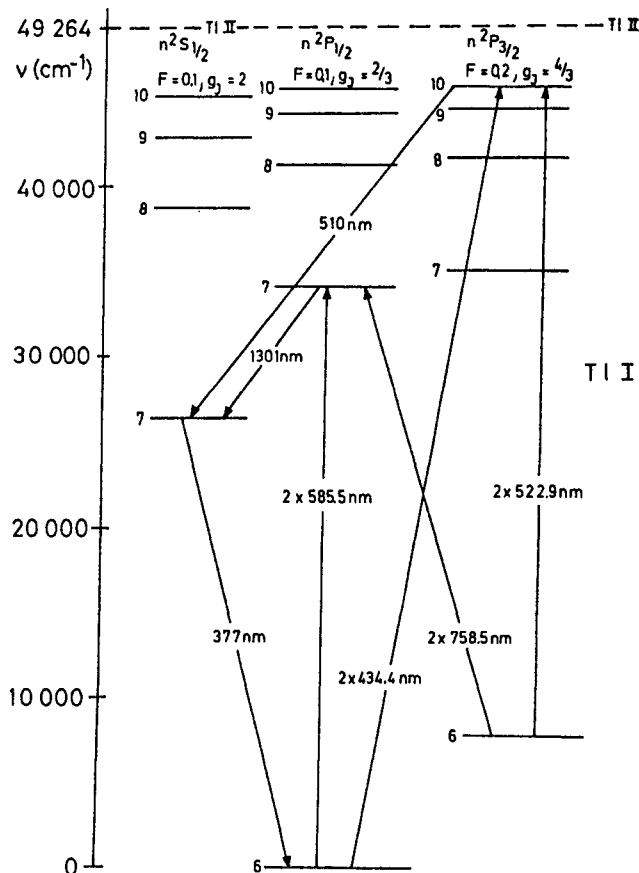


FIG. 1. Thallium energy-level diagram.

values agree well with results ($nP_{3/2}$, $n = 8-11$) measured by two-photon excited hyperfine level-crossing spectroscopy.¹¹ The complete measurement of this line series gives reliable information about the level IS by extrapolation to the series limit and about the systematic behavior of HFS and the IS in the $nP_{1/2,3/2}$ series ($n = 7-10$).

II. EXPERIMENTAL SETUP

The experimental setup is shown in Fig. 2. An actively stabilized single-mode cw dye ring laser (Spectra 380D) is used, providing an effective linewidth of less than 1 MHz rms. The original galvo drive in the reference interferometer of the laser system was replaced by a type of lower gain drift and zero drift (General Scanning G 306), driven by a home-built output stage in combination with the standard control circuit. Thus a better scan linearity at slow scan rates over small frequency ranges (typically 1.5 GHz/10 min) could be achieved. Doppler-free two-photon absorption is enabled by the well-known arrangement with counterpropagating waves. A corner cube prism is used as reflector. A Faraday rotator serving as optical isolator prevents feedback into the laser system.

The thallium is vaporized in an oven-heated quartz cell, which remains connected to a vacuum and gas-filling system via a quartz valve. The cell and valve are heated to temperatures up to 900 °C. This arrangement, also being used for measurements of pressure broadening and shift¹² by noble gases, allows all outgassed impurities from the cell to be pumped out and ensures constant signal quality.

Precise scan calibration has been obtained by use of a marker-cavity (free spectral range 150.87 MHz), which was actively stabilized¹³ by means of an I₂-referenced He-Ne laser, giving a long-term absolute stability of the frequency reference marks of about 1 MHz. The absorption wavelengths were monitored by a homemade digital-reading wave meter (Kowalski-type interferome-

ter, 1-GHz resolution). The two-photon absorption was measured by detection of the fluorescence on a resonance transition in the cascade ($7S_{1/2}-6P_{1/2}$, $\lambda = 377$ nm). The fluorescence signal and the transmission of the marker cavity were recorded simultaneously, digitized (12-bit resolution) and stored by a microcomputer used as 4096-channel analyzer and as a scan-control unit of the dye-laser spectrometer. The dye-laser frequency was modulated (modulation frequency 272 Hz, amplitude of modulation in the optical spectrum 2.1 MHz rms) and signal-to-noise improvement was achieved by use of lock-in amplifiers.

III. MEASUREMENTS AND RESULTS

The wave-meter measurements of the absorption wavelengths were according to the energies given by Moore,¹ except for the $10P_{1/2}$ and $11P_{1/2}$ level. We found $45\,941.6 \pm 0.4$ cm⁻¹ for the level energy of $10P_{1/2}$ and $46\,856.5 \pm 0.4$ cm⁻¹ for $11P_{1/2}$ and the fine-structure splitting of the $10P_J$ states is 102.0 ± 0.2 cm⁻¹ instead of 104.3 cm⁻¹ as tabulated.¹

Two-photon transitions into states with $n = 7$ (R6G as the laser dye) and $n = 10$ (Stilben 3) were excited from the ground state, but for $n = 8$ (R6G) and $n = 9$ (R110) they were excited from the metastable state $6P_{3/2}$ because the laser dyes for the two-photon excitation wavelengths of $6P_{1/2}-8,9P_J$ transitions show poor performance (low power, short lifetimes). Only the $6P_{1/2}-9P_{1/2}$ transition can still be excited by use of Stilben 3 as laser dye. The $6P_{3/2}$ level lying 7793 cm⁻¹ above the ground state is thermally populated (10^{12} atoms/cm³ at 850 °C, i.e., about 10^{-4} of the particle density in the ground state). The two-photon transitions used in this work as well as the excitation wavelengths and the laser powers employed are listed in Table I.

The two-photon absorption spectra were calibrated by

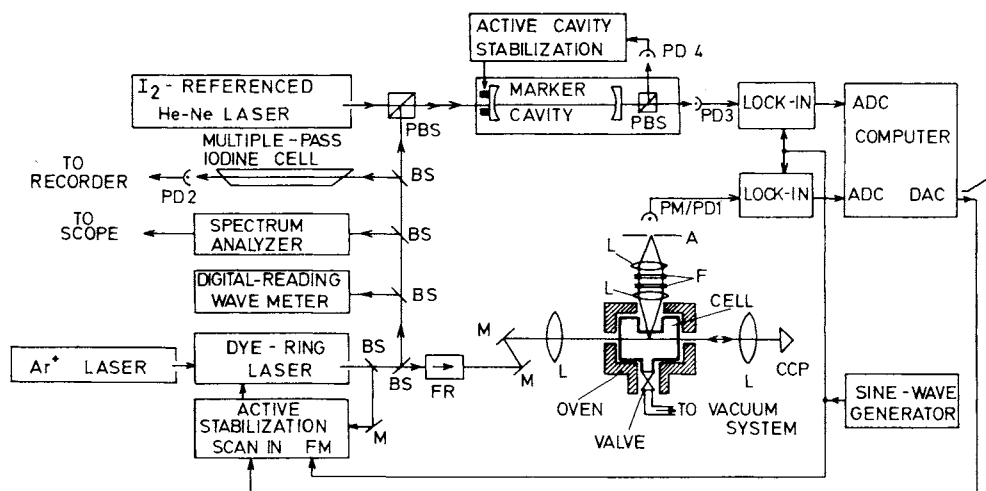


FIG. 2. Experimental setup. BS, beam splitter; CCP, corner cube prism; F, optical filter; A, aperture; FR, Faraday rotator; PBS, polarizing beam splitter used as beam combiner; PD, photodiodes; PM, photomultiplier; ADC, DAC, analog-to-digital and digital-to-analog converters.

TABLE I. Excitation wavelengths, laser dyes, and laser powers used for spectroscopy of two-photon transitions in thallium.

Two-photon transition	Dye	λ_{exc} (nm)	P_{dye} (mW)	P_{pump} (W)
$6P_{1/2}-7P_{1/2}$	R6G	585.5	800	4 (514 nm)
$6P_{1/2}-7P_{3/2}$	R6G	568.8	500	4 (514 nm)
$6P_{3/2}-8P_{1/2}$	R6G	595.7	1300	8 (514 nm)
$6P_{3/2}-8P_{3/2}$	R6G	589.1	1300	8 (514 nm)
$6P_{1/2}-9P_{1/2}$	S3	450.6	80	3 (uv)
$6P_{3/2}-9P_{1/2}$	R110	546.6	1000	8 (514 nm)
$6P_{3/2}-9P_{3/2}$	R110	543.9	900	8 (514 nm)
$6P_{1/2}-10P_{1/2}$	S3	435.3	190	3 (uv)
$6P_{1/2}-10P_{3/2}$	S3	434.4	180	3 (uv)
$6P_{1/2}-11P_{1/2}$	S3	426.8	80	3 (uv)

the marker cavity. A typical spectrum is shown in Fig. 3 and the results for the HFS are listed in Table II. The noted errors are statistical errors (standard deviations) calculated from a number (5–14) of scans over each hyperfine transition. The errors are mainly due to a residual nonlinearity of the laser scan.

For calculation of the isotopic level shifts from the line shifts one has to refer to a level of the known IS. In the first step of evaluation we choose the ground state as the reference level. A plot of these shifts versus n^{*-3} is given in Fig. 4. A linear extrapolation to $n^{*-3}=0$ (ionization limit) gives an isotopic shift of the ionization limit of 1255 MHz related to a zero ground-state shift. This means a shift of -1255.0 MHz in the ground state relat-

TABLE II. Hyperfine splittings of n^2P_J states in $^{203,205}\text{Tl}$. Values are from this work if not otherwise noted.

Level nP_J	Hyperfine splitting (MHz)	
	^{203}Tl	^{205}Tl
$6P_{1/2}$	$21\,105.4 \pm 0.0^{\text{a}}$	$21\,310.8 \pm 0.0^{\text{a}}$
$6P_{3/2}$	$524.1 \pm 0.0^{\text{b}}$	$530.1 \pm 0.0^{\text{b}}$
$7P_{1/2}$	2134.6 ± 0.8	2155.5 ± 0.6
$7P_{3/2}$	617.3 ± 0.5	622.8 ± 0.6
$8P_{1/2}$	781.7 ± 1.6	788.5 ± 0.9
$8P_{3/2}$	260.2 ± 0.9	260.4 ± 1.1
$9P_{1/2}$	375.4 ± 0.6	378.4 ± 0.8
$9P_{3/2}$	132.5 ± 0.6	134.2 ± 0.5
$10P_{1/2}$	216.6 ± 1.4	221.7 ± 2.2
$10P_{3/2}$	76.9 ± 0.7	78.5 ± 0.3
$10P_{3/2}$	$77.6 \pm 0.3^{\text{c}}$	$79.2 \pm 0.3^{\text{c}}$
$10P_{3/2}$		$77.7 \pm 0.7^{\text{d}}$
$11P_{3/2}$		$48.8 \pm 0.5^{\text{d}}$
$12P_{3/2}$		$32.3 \pm 0.5^{\text{d}}$
$13P_{3/2}$		$23.1 \pm 0.4^{\text{d}}$

^aFrom Ref. 2.

^bFrom Ref. 3.

^cFrom Ref. 7; values given there have to be corrected by a factor of 2 [Ref. 7(b)].

^dFrom a previous work (Ref. 8).

ed to the ionization limit. Subtraction of this value from the previously calculated shifts of all other levels yields the isotopic shifts with respect to the ionization limit as tabulated in Table III. In addition the contributions by normal mass effect are given in this table.

IV. DISCUSSION

A. Hyperfine structure

The most convenient discussion of HFS and the IS has been done on the basis of semiempirical relativistic

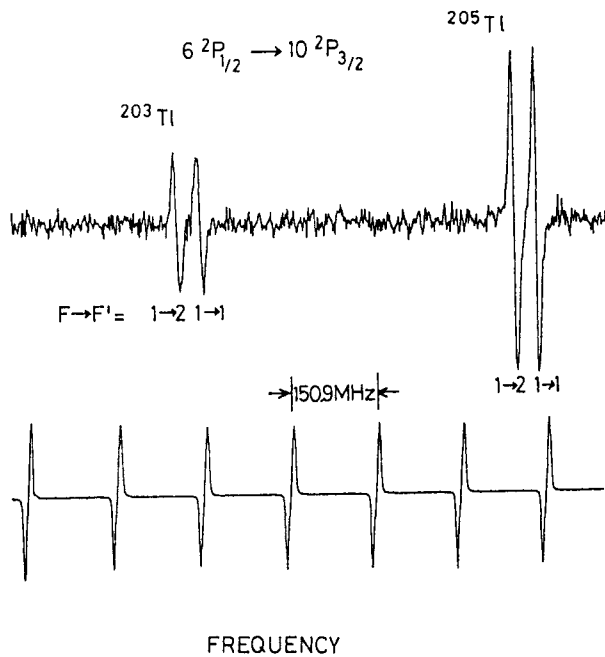


FIG. 3. Typical two-photon spectrum of the $6P_{1/2} \rightarrow 10P_{3/2}$ transition, recorded at 980 K; laser power 180 mW at 434.4 nm. Upper trace, fluorescence signal of the $7S_{1/2} \rightarrow 6P_{1/2}$ resonance transition ($\lambda=377$ nm). Lower trace, frequency reference marks.

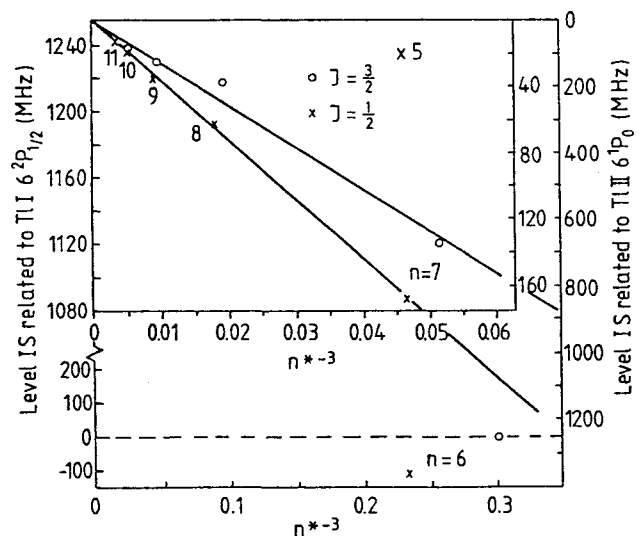


FIG. 4. Isotopic level shifts related to ground state and to the ionization limit, vs n^{*-3} .

TABLE III. Isotopic level shifts relative to the ionization limit, contributions due to the normal-mass effect (NME), electron density at the nucleus $|\psi(0)|^2$, and differences to the ionization limit for the n^2P_J states in Tl.

Level	Level shift (MHz)	NME (MHz)	$4\pi \psi(0) ^2/a_0^{-3}$	$(4\pi\Delta \psi(0) ^2)/a_0^{-3}$
Tl I				
$6P_{1/2}$	-1255.0 ± 0.1	38.7	31 412 631.6	-415.0
$6P_{3/2}$	-1356.4 ± 1.2	32.6	2601.8	-444.8
$7P_{1/2}$	-134.8 ± 1.0	11.9	3025.1	-21.5
$7P_{3/2}$	-167.9 ± 0.8	11.1	3007.8	-38.8
$8P_{1/2}$	-37.2 ± 1.2	6.2	3038.9	-7.7
$8P_{3/2}$	-61.8 ± 2.9	5.9	3032.4	-14.2
$9P_{1/2}$	-24.8 ± 0.9	3.8	3042.6	-4.0
$9P_{3/2}$	-34.8 ± 2.1	3.7	3039.4	-7.2
$10P_{1/2}$	-16.0 ± 1.6	2.6	3044.0	-2.6
$10P_{3/2}$	-18.1 ± 1.2	2.5	3042.3	-4.3
$11P_{1/2}$	-13.1 ± 1.9	1.9	3044.8	-1.8
$\lim_{n^* \rightarrow 0} n^* \rightarrow 0$			3046.6	0
Tl II	$6s^2$		3045.1	

theory.¹⁴⁻¹⁶ The A_J factors of magnetic hyperfine interaction are given by

$$A(^2P_J) = l(l+1)/[j(j+1)]a_p F_r(j, Z_i) \times (1-\epsilon)(1-\delta), \quad (1)$$

where a_p represents the orbital contribution, which can be expressed by the effective quantum number n^* :

$$a_p = \frac{2(\mu_0/4\pi)\mu_I\mu_B Z_a^2 Z_i}{\hbar l(l+1)(l+1/2)a_0^3 n^{*3}}, \quad (2)$$

where $F_r(j, Z_i)$ is the relativistic correction,¹⁵ $(1-\epsilon)(1-\delta)$ are volume corrections: $(1-\epsilon)(1-\delta) = 0.9624$ for $nP_{1/2}$ states, following Rosenberg and Stroke,¹⁷ Z_i is the shielded nuclear charge ($Z_i \approx Z - 4$ for p electrons¹⁵), $Z_a = 1$ for neutral atoms, a_0 is the Bohr radius, μ_B is the Bohr magneton, and $\mu_I = g_I \mu_K$, the nuclear magnetic moment, with $g_I = 3.27643$ for ²⁰⁵Tl.¹⁸

The semiempirical theory predicts a linear relation between the hyperfine splitting and the effective quantum number n^{*-3} :

$$A_{\text{theor}}(nP_{1/2}) \text{ (MHz)} = 36784n^{*-3}, \quad (3)$$

$$A_{\text{theor}}(nP_{3/2}) \text{ (MHz)} = 4166n^{*-3}$$

(dashed lines in Fig. 5). For $P_{1/2}$ states one gets a good accordance with the line fitted to the experimental data for levels with $n \geq 7$ (solid line in Fig. 5), assuming a $Z_i = 80.5$, i.e., higher than usual.¹⁵ On the other hand, the even greater disagreement with the experimental data for $P_{3/2}$ states cannot be overcome by the assumption of a higher Z_i . In this model the ratio $A(nP_{1/2})/A(nP_{3/2})$ is determined mainly by the relativistic correction F_r .¹⁵ In addition there are large deviations of the measured values for the $6P_J$ levels from the least square fits for $n \geq 7$. They may be interpreted as a result of configuration interactions at the $6P_J$ states. Such configuration interactions in the case of thallium have been discussed in the literature^{15,16} since the early work of Fermi and Segre.¹⁹ The HFS values for the $P_{1/2}$ and

$P_{3/2}$ series being measured with high accuracy are lying on a smooth curve which can be fitted precisely by $A_J = \alpha_J n^{*-3} + \beta_J n^{*-6}$. The agreement of such a fit is not very surprising since most static and magnetic interactions of the valence electron with a localized core scale with n^{*-3} .

Ab initio Dirac-Fock (DF) calculations²⁰ have been carried out by one of us for some of the n^2P_J states giving the radial integrals

$$F_{ii'} = \{-2/[\alpha a_0(k+k'+2)]\} \times \int_0^\infty [P_i(r)Q_{i'}(r) + P_{i'}(r)Q_i(r)]r^{-2}dr, \quad (4)$$

where $P_i(r)$ and $Q_i(r)$ are the large and small components of the Dirac wave functions, respectively, i, i' stand for $J = 1/2$ and $J = 3/2$, respectively; $k = 1$ for $J = 1/2$ and $k = -2$ for $J = 3/2$.

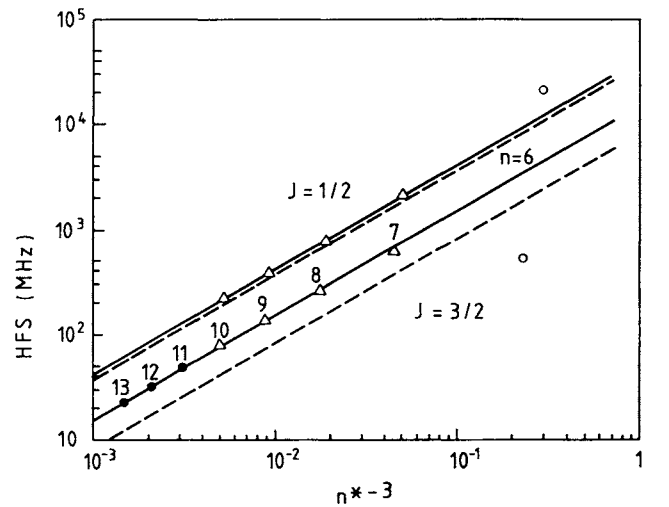


FIG. 5. Hyperfine splittings in Tl as a function of n^{*-3} . Δ , experimental values from this work; \bullet , from a previous work (Ref. 8); \circ , values from other authors (Refs. 2 and 3); ---, semiempirical theory; —, fit to data for $n \geq 7$.

From these integrals the radial parameters and the HFS constants can be derived using the effective operator formalism by Sandars and Beck.^{21,22} Assuming *LS* coupling the hyperfine constants for ²⁰⁵Tl ($g_I = 3.27643$) (Ref. 18) can be calculated for *p* states from

$$A_J = \frac{4(\mu_0/4\pi)\mu_I\mu_B}{hIJ(J+1)} F_{J,J'}, \quad (5)$$

$$\begin{aligned} A_{1/2} \text{ (MHz)} &= 820.096F_{1/2,1/2}/a_0^{-3}, \\ A_{3/2} \text{ (MHz)} &= 164.019F_{3/2,3/2}/a_0^{-3}, \end{aligned} \quad (6)$$

and the radial parameters in the common form are given by

$$\langle r^{-3} \rangle_l = \frac{1}{9}(4F_{3/2,3/2} + F_{3/2,1/2} + 4F_{1/2,1/2}), \quad (7)$$

$$\langle r^{-3} \rangle_{sd} = \frac{1}{27}(-8F_{3/2,3/2} - 5F_{3/2,1/2} + 40F_{1/2,1/2}), \quad (8)$$

$$\langle r^{-3} \rangle_s = \frac{8}{27}(2F_{3/2,3/2} - F_{3/2,1/2} - F_{1/2,1/2}). \quad (9)$$

Additionally, some multiconfiguration DF calculations were carried out to test the influence of configuration interactions for the $6P_J$ states. In particular, the following configurations interacting with the ground-state

configuration were successfully calculated: (a) $5d^86s^27s^26p$, (b) $5d^86s^26p$, and (c) $5d^{10}6p^3$. One-electron excitations are taken into account by every DF calculation by itself (Brillouin theorem). Table IV gives a compilation of the values for the radial parameters of the resulting theoretical hyperfine constants from this work and of the data from semiempirical theory as well as from relativistic Hartree-Fock calculations.²² It turns out that the semiempirical theory as well as the DF calculations are able to give values for the HFS in the $nP_{1/2}$ states in satisfactory agreement with experimental data except of the ground state $6P_{1/2}$. Here DF calculations improve the predictions of the semiempirical theory and reduce the difference by about 75%. Results of further calculations show that the influence of the investigated configuration interactions is small compared with the deviations of the $6P_{1/2}$ state.

On the other hand, neither semiempirical theory nor DF calculations give the correct HFS in the $nP_{3/2}$ series. Each of the calculated values for $n \geq 7$ is too small, approximately by a factor of 2, in comparison with experimental data. Significant differences between semiempirical theory and DF calculation in the *P*-term series are found for the $6P_{3/2}$ state only, but unfortunately, here the result of the DF calculations enlarges the difference

TABLE IV. *Ab initio* ratio integrals and resulting hyperfine constants of ²⁰⁵Tl in comparison with experiment and semiempirical theory.

	$\langle r^{-3} \rangle_l/a_0^{-3}$	$\langle r^{-3} \rangle_{sd}/a_0^{-3}$	$\langle r^{-3} \rangle_s/a_0^{-3}$	$A_{1/2}$ (MHz)	$A_{3/2}$ (MHz)
6P_J					
Experimental				21 310.8	265.1
Semiempirical ^a				11 072	967
HF ^b	15.159	29.860	-4.910	18 964	1380
OHFS ^b	14.339	30.359	-5.479	18 890	1133
DF ^c	15.886	28.031	-7.084	18 734	1381
DF + Config. 1 ^d	17.555	25.824	-11.076	18 922	1405
DF + Config. 2 ^e	15.890	28.014	-7.071	18 728	1384
DF + Config. 3 ^f	15.920	28.002	-6.421	18 668	1458
RHF + Pol. + Corr. ^g				21 315	599
<i>g</i> -H ^h				20 894	895
7P_J					
Experimental				2155.5	311.4
Semiempirical ^a				1879	192
DF ^c	1.745	2.832	-0.555	1933	185
RHF + Pol. + Corr. ^g				2039	384
8P_J					
Experimental				788.5	130.2
Semiempirical ^a				724	75
DF ^c	0.620	1.045	-0.225	706	61

^aUsing $Z_i = 77$ and relativistic correction factors (Ref. 15).

^bHartree-Fock and optimized Hartree-Fock-Slater (Ref. 22).

^cDirac-Fock (this work).

^dMulticonfiguration $5d^{10}6s^26p + 5d^86s^26p^3$ (this work).

^eMulticonfiguration $5d^{10}6s^26p + 5d^86s^26p7s^2$ (this work).

^fMulticonfiguration $5d^{10}6s^26p + 5d^{10}6p^3$ (this work).

^gRelativistic Hartree-Fock with polarization and correlation corrections (Ref. 25).

^h*g*-Hartree calculations (Ref. 26).

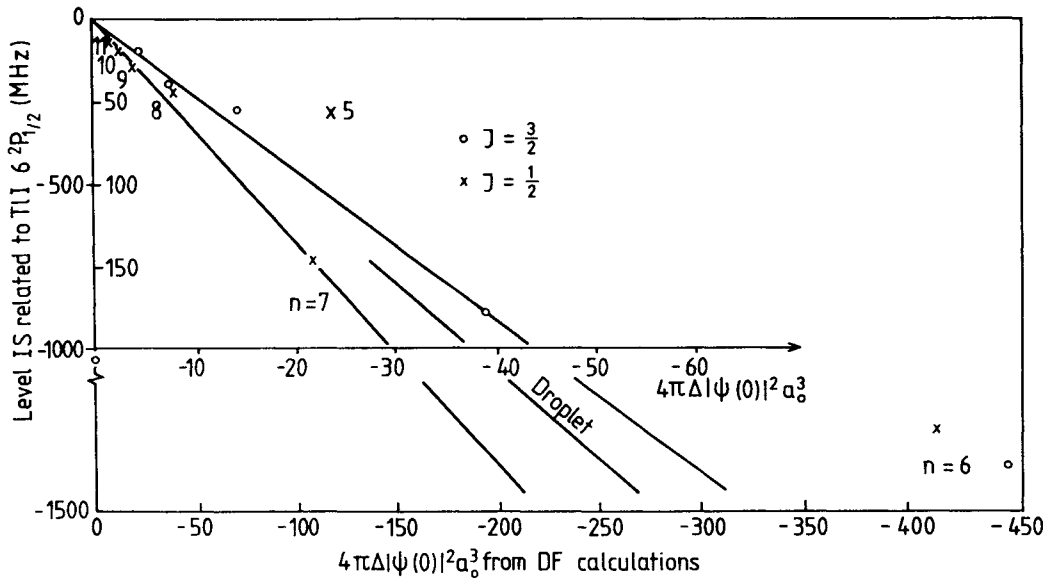


FIG. 6. Experimental isotopic level shifts as a function of the electron density at the nucleus $|\psi(0)|^2$ referred to the ionization limit. The straight lines are least-square fits of the experimental data for $n \geq 7$ of the $nP_{1/2}$ and $nP_{3/2}$ series, respectively; additionally, the slope given by the droplet model (Ref. 24) is drawn. Multiconfiguration DF calculations for $6P_J$ give the following: $6P_{1/2}$, $4\pi\Delta|\psi(0)|^2 = -528.6/a_0^{-3}$; $6P_{3/2}$, $4\pi\Delta|\psi(0)|^2 = -579.7/a_0^{-3}$.

to the experimental value compared with the semiempirical theory. This disagreement of the DF calculations points to a interaction of a double excited state, which has not been calculated up to now (e.g., $5d^9 6s 6p^3$).

B. Isotopic shift

For the interpretation of the isotopic shift data one has to separate the level shift contributions due to field shift and mass effect. The normal-mass effect (NME) has been taken into account; nevertheless it is small compared with the field shift. It has been assumed that omission of the specific mass effect causes no essential error, since specific mass effects comparable or larger than the NME have been observed only in electronic configurations with partially filled inner shells.^{23,24} Therefore the difference between measured isotopic level shift and the NME in the case of thallium has been regarded as due to the field shift, which is given by

$$\Delta E = (4\pi\epsilon_0)^{-1} (2/3\pi e^2 Z) |\psi(0)|^2 \delta\langle r^2 \rangle. \quad (10)$$

$\delta\langle r^2 \rangle$ is the difference of the mean square radii of the two isotopes and $|\psi(0)|^2$ is the total electronic density at the nucleus. The electronic density at the nucleus has been calculated *ab initio* by the relativistic Dirac-Fock method. Figure 6 shows a plot of the experimental isotopic shift data versus these results for the nP_J series. The straight lines given in this figure are least-square fits for $nP_{1/2}$ and $nP_{3/2}$ states, respectively. From the slope of these lines $\delta\langle r^2 \rangle$ may be calculated. One finds that from $nP_{1/2}$, $\delta\langle r^2 \rangle = 0.211 \text{ fm}^2$; from $nP_{3/2}$, $\delta\langle r^2 \rangle = 0.143 \text{ fm}^2$; and from the droplet model, $\delta\langle r^2 \rangle = 0.169 \text{ fm}^2$. The calculations give the correct linear relation between isotopic shift and $|\psi(0)|^2$ within both nP_J series for $n \geq 7$, but there is a systematic discrepancy between the values for the $nP_{1/2}$ and $nP_{3/2}$ series, respectively. Since the calcu-

lated electronic densities for $6P_J$ are much smaller than expected from Fig. 6 (about 150 a.u.), it points to the fact that either the screening of the $6s$ electrons by the p electron is overrated by the present calculations or an additional double excited configuration has to be considered.

V. CONCLUSIONS

Experimental data of hyperfine splittings and isotopic shifts in the n^2P_J series of thallium have been measured for the first time or with far-enhanced accuracy. The complete line series allows the extrapolation to the series limit and, thus, reliable determination of the level IS. These data were compared with the results of semiempirical and new *ab initio* Dirac-Fock calculations.

The agreement of DF calculations with experimental data is satisfactory in the $nP_{1/2}$ series. However, there remains a discrepancy of approximately a factor of 2 in the results of DF calculations as well as in the semiempirical theory for the $nP_{3/2}$ series ($n \geq 7$). Even configuration interactions of the calculated types (Table III) could not explain the HFS's of the $6P_J$ states.

The analysis of the IS data in comparison to the DF values for electron densities shows that—similar to the situation in the HFS—the systematic behavior within each term series is reproduced by the theory. However a discrepancy also remains between the $J = \frac{1}{2}$ and $J = \frac{3}{2}$ term series.

ACKNOWLEDGMENTS

The authors gratefully acknowledge many helpful discussions and generous support from Dr. A. Scharmann. This work has been supported by the Deutsche Forschungsgemeinschaft (Bonn, Federal Republic of Germany).

- ¹C. E. Moore, *Atomic Energy Levels*, Natl. Bur. Stand. (U.S.) Circ. No. 467 (U.S. GPO, Washington, D.C., 1958), Vol. III, pp. 202–203.
- ²A. Lurio and A. G. Prodell, *Phys. Rev.* **101**, 79 (1956).
- ³F. R. Petersen, H. G. Palmer, and J. H. Shirley, *Bull. Am. Phys. Soc.* **13**, 1674 (1968).
- ⁴A. I. Odintsov, *Opt. Spektrosk.* **9**, 142 (1960) [*Opt. Spectrosc. (USSR)* **9**, 75 (1960)].
- ⁵C. J. Schuler, M. Ciftan, L. C. Bradley, III., and H. H. Stroke, *J. Opt. Soc. Am.* **52**, 501 (1962).
- ⁶A. Flusberg, T. Mossberg, and S. R. Hartmann, *Phys. Rev. A* **14**, 2146 (1976).
- ⁷(a) K. H. Weber, J. Lawrenz, A. Obrebski, and K. Niemax, *Phys. Scr.* **35**, 309 (1987); (b) K. Niemax (private communication).
- ⁸G. Hermann, H.-O. Irmeler, G. Lasnitschka, and A. Scharmann, *Z. Phys. D* **3**, 397 (1986).
- ⁹M. Grexa, G. Hermann, G. Lasnitschka, and A. Scharmann, *Z. Phys. D* **2**, 157 (1986).
- ¹⁰M. Grexa, Ph.D. thesis, Justus-Liebig-Universität, Giessen, 1987.
- ¹¹G. Hermann, G. Lasnitschka, J. Richter, and A. Scharmann, *Z. Phys. D* (to be published).
- ¹²M. v. Borstel, G. Hermann, G. Lasnitschka, and A. Scharmann, *Z. Phys. D* **9**, 15 (1988).
- ¹³M. Mahr, Diplom thesis, Justus-Liebig-Universität, Giessen, 1987.
- ¹⁴H. B. G. Casimir, *On the Interaction between Atomic Nuclei and Electrons* (Freeman, New York, 1963).
- ¹⁵H. Kopfermann, *Kernmomente* (Akademische Verlagsgesellschaft, Frankfurt, 1956).
- ¹⁶W. Fischer, *Fortschr. Phys.* **18**, 89 (1970).
- ¹⁷H. J. Rosenberg and H. H. Stroke, *Phys. Rev. A* **5**, 1992 (1972).
- ¹⁸F. Kohlrausch, *Praktische Physik* (Teubner, Stuttgart 1986), Vol. 3.
- ¹⁹S. Fermi and E. Segre, *Z. Phys.* **82**, 729 (1933).
- ²⁰J.-P. Declaux, *Comput. Phys. Commun.* **9**, 31 (1985).
- ²¹P. G. H. Sandars and J. Beck, *Proc. R. Soc. London, Ser. A* **289**, 97 (1965).
- ²²I. Lindgren and A. Rosen, in *Case Studies in Atomic Physics IV*, edited by E. W. McDaniel and M. R. C. McDowell (North-Holland, Amsterdam, 1975).
- ²³W. H. King, *Isotope Shifts in Atomic Spectra* (Plenum, New York, 1984).
- ²⁴L. R. B. Elton, *Nucl. Phys.* **5**, 173 (1957).
- ²⁵A. Dzuba, V. V. Flambaum, P. G. Silvestrov, and O. P. Sushkov, *J. Phys. B* **20**, 1399 (1987).
- ²⁶T. Millack, *Z. Phys. D* **8**, 119 (1988).